JOURNAL OF CATALYSIS 105, 285–298 (1987)

The Generation of Brønsted and Lewis Acid Sites on the Surface of Silica by Addition of Dopant Cations

GLEN CONNELL[1] AND J. A. DUMESIC[2]

Department of Chemical Engineering, University of Wisconsin, Madison, Wisconsin 53706

Received March 23, 1986; revised January 6, 1987

Pyridine adsorption was used to study the acidic properties of silica doped with the following cations: Sc^{3+}, Mg^{2+}, Fe^{2+}, Fe^{3+}, Zn^{2+}, Al^{3+}, and Ga^{3+}. All samples were exposed to pyridine at 423 K and subsequently evacuated at successively higher temperatures to 723 K. Infrared spectra of the adsorbed pyridine indicated that all of these cations generated Lewis acid sites. This can be explained by the presence of coordinatively unsaturated dopant cations on the surface of silica, in accord with a model based on Pauling's electrostatic bond strength rules. The infrared frequency of the 19b band of pyridine adsorbed on these Lewis acid sites was found to increase with increasing electronegativity of the dopant cation. It is suggested that both of these quantities are related to the strength of the Lewis acid sites. Brønsted acid sites were also observed by infrared spectroscopy for Sc^{3+}, Al^{3+}, and Ga^{3+} on silica. These dopant cations are believed to be bonded tetrahedrally on the surface of silica, generating bridging hydroxyl groups between the dopant cation and Si^{4+}. As for zeolite catalysts, the proton associated with these groups and required for charge neutrality is the Brønsted acid site. Finally, Brønsted acid sites can also be generated on silica by highly electronegative anions, such as HPO_4^{2-}, which generate Brønsted acidity in a different manner.

INTRODUCTION

Metal oxide catalysts are of importance for a number of industrial processes, such as catalytic cracking, partial oxidation, and dehydration (*1–3*). In general, the catalytic properties of this class of materials can be expected to be influenced by the number, type, and strength of the acid sites on the surface. For example, very weak acid sites may not be active catalytically while very strong acid sites may lead to excessive cracking and carbon deposition. In addition, the catalytic properties of Brønsted acid sites (proton donors) may well be different from those of Lewis acid sites (electron pair acceptors). For example, it has been suggested that Brønsted acids are much more active than Lewis acids for skeletal transformations of hydrocarbons (*3*). It is thus of importance to understand the factors that determine the strength and type of acid sites on metal oxide catalysts; this is the objective of the present study of silica-supported metal oxides.

Lewis acid sites have been observed on a wide variety of mixed metal-oxide systems (*4–16*); in contrast, Brønsted acid sites have been observed on a limited number of mixed metal oxides, perhaps the best example being that of silica–alumina catalysts (*3, 4, 11*). Similarly, Lewis acid sites have been detected on a number of single-component metal oxides (*17–33*), whereas Brønsted acid sites have not to our knowledge been found on pure oxides free of additives such as P, Cl, and S. The results of the present paper explain these observations, and a model is presented that explains the type of the acid site and the relative strength of the Lewis acid sites on a series of silica-supported metal oxides. In short, this model involves the electronegativity and coordination of the metal cations on the silica surface.

Although there have been many previous studies of the acidity of mixed-metal ox-

[1] Present address: 3M Center, St. Paul, MN 55144.
[2] Author to whom correspondence should be addressed.

0021-9517/87 $3.00

ides, there have been few systematic studies on a series of related materials. In addition, the nature of acidity is such that its definition is related to the methods used to measure it. Hence, it was felt necessary to conduct a systematic study on a series of model materials to understand the acidic properties of these materials. It was shown in previous papers in this series (*34, 35*) that the surface of silica is well suited for supporting unsaturated cations. In addition, silica alone has little to no acidity, and changes in acidity can be observed and can be attributed to the added, second component.

The materials used in this study are in the regime of dilute binary oxides; i.e., they each contain two components with the major component controlling the structure. In addition, the minor oxide component is expected to be located near the surface, since these materials were prepared by impregnation of this component onto the silica surface (*34*). Hence, these materials can be used to model in an approximate manner the interaction of individual cations with a host oxide structure. One would assume that these types of sites might also occur on the surface of true binary oxides, which will in general have a different bulk structure.

The dopant metal cations chosen for study were Sc, Mg, Fe, Zn, Al, Ga, and P. The number of acid sites formed by depositing these oxides on silica was determined by gravimetric measurements of pyridine adsorption. The type and strength of the acid sites were monitored through analysis of infrared spectra of adsorbed pyridine.

EXPERIMENTAL

Sample Preparation

All samples were prepared by incipient wetness impregnation utilizing 1 ml of solution per gram of SiO_2. The silica (Cab-O-Sil grade S-17) was X-ray amorphous with a surface area of 400 m^2/g. All metal-doped samples (Sc, Mg, Fe, Zn, Al, and Ga) were prepared using nitrate salts followed by heating in air at 400 K. The samples were then treated in H_2 at 723 K for 4 h (except for Fe at 673 K) followed by oxidation in O_2 at 723 K (except for Fe at 423 K). The sample containing P was prepared with a $(NH_4)H_2PO_4$ solution and only subjected to oxidation at 723 K. The samples were chemically analyzed by Galbraith Laboratories to determine the actual loadings. These loadings along with the electronegativities and sizes of the cations are listed in Table 1. It should be noted that P_2O_5 should have a vapor pressure of 760 Torr at 575 K, and if this bulk phase were present it would have volatilized under the oxidation treatment. The loading of P, however, was within error of the added amount during impregnation, indicating that the phosphorous oxide was stabilized on the SiO_2 surface.

Experimental Procedure

The acidic properties of these mixed oxides were studied using pyridine adsorp-

TABLE 1

Summary of Properties of the Dopants Used on SiO_2

Dopant	Loading[a]	EN[b]	CN[c]	Size[d] (pm)
Sc^{3+}	18.4	3.02	6	68[e]
Mg^{2+}	14.2	3.22	4	71
			6	86
Fe^{2+}	14.0	3.33	4	77
			6	92
Fe^{3+}	14.0	3.62	4	63
			6	78.5
Al^{3+}	14.5	3.72	4	53
			6	67.5
Zn^{2+}	12.0	3.85	4	74
			6	88
Ga^{3+}	12.3	4.30	4	61
			6	76
P^{5+}	13.6	4.59	4	31
			6	52
SiO_2	800	4.14	4	40
			6	54

[a] Loading in units of cations/$m^2 \times 10^{16}$.
[b] Sanderson electronegativity of the oxide (*36*).
[c] Coordination number.
[d] From Ref. (*37*).
[e] From Ref (*38*).

tion. The number of acid sites was determined using gravimetric adsorption measurements. The type of the site (Lewis versus Brønsted) and site strength distribution were probed using infrared spectroscopy of adsorbed pyridine. The pyridine used in these experiments was Mallendrockt Spectrophotometric grade. It was stored over activated 3A molecular sieve and degassed with the freeze–pump–thaw technique.

The sample treatments employed in this study (and described in the following two sections) were chosen to ensure a consistent state of surface dehydration and incorporation of the dopant cations into the silica surface. This procedure was developed in study of iron deposited onto silica, where Mössbauer spectroscopy could be used to monitor the state of iron on the surface (*34*); and, for consistency, we have used the same treatments for all samples.

Since the highest treatment temperature used in this study was 773 K, one would expect there to be a large number of hydroxyl groups on the silica surface that may react with the dopant cations to form various types of acidic sites. As mentioned earlier, acidity is defined by the process used to measure it. For the purpose of this study, the number of acid sites is the number of sites that are capable of irreversibly adsorbing pyridine at 423 K. Whether the sites are Brønsted or Lewis depends on the infrared spectrum of this irreversibly adsorbed pyridine at this temperature. Note that acidity was not measured or defined at lower temperatures where a large amount of weakly adsorbed pyridine is present.

Gravimetric Adsorption Measurements

The gravimetric adsorption measurements of pyridine were accomplished using a quartz-spring balance (Worden). The spring was suspended in a Pyrex tube that was water jacketed to maintain a constant temperature. The sample (typically 400 mg in weight) was pressed into a pellet for ease of handling and was placed into a quartz pan which was suspended from the quartz spring in a Pyrex section. This section had a furnace surrounding it to carry out temperature treatments. The top of the water-jacketed chamber was connected to a diffusion-pumped vacuum system. A 13X molecular sieve trap held at 77 K was also connected to the system near the sample to aid in the evacuation of pyridine from the system.

Prior to pyridine adsorption measurements, the samples were reduced in flowing H_2 at 723 K for 4 h, evacuated, and oxidized at 723 K in flowing O_2 for another 4 h. The sample was next evacuated until a pressure of 5×10^{-5} Torr was achieved, as measured with an ionization gauge close to the inlet to the diffusion pump. The sample was then cooled to 423 K in a dynamic vacuum and equilibrated with pyridine at 4.8 Torr (which is the vapor pressure of pyridine at 273 K). The equilibration was carried out for 1 h, even though the sample weight became constant after 0.3 h. The sample was then evacuated at 423 K until the pressure of pyridine was below 3×10^{-5} Torr. This pressure was achieved in 5 h, but evacuation was carried out overnight to ensure complete desorption of physisorbed pyridine.

The maximum number of acid sites was taken from the sample weight gain upon adsorption and subsequent evacuation of pyridine at 423 K. The sample temperature was then raised sequentially to 523, 623, and 723 K, with evacuation at each temperature to a pressure of 3×10^{-5} Torr or 1 h, whichever took longer. These data probe the acid strength distribution.

Infrared Spectroscopy

Infrared spectra of adsorbed pyridine were collected with a Nicolet 7199 Fourier transform infrared spectrometer. The sample was pressed into a pellet and placed in a cell in which the sample could be moved from a Pyrex section where heat treatments occurred, to an aluminum section with CaF_2 windows for collection of spectra. The sample treatments, exposure to pyri-

dine, and evacuations were identical to the gravimetric adsorption measurements described above. The only difference was that the pressure achieved during evacuation of pyridine was typically 2×10^{-4} Torr. In addition, a spectrum was collected for each sample in a pyridine pressure of ca. 1×10^{-3} Torr to illustrate the position of the bands due to physisorbed pyridine.

All infrared spectra were collected at room temperature. Purified He was used in the cell to act as a heat transfer medium to facilitate the cooling and heating of the samples. All spectra reported have had the spectrum of the sample, after treatment but prior to pyridine adsorption, subtracted from the obtained spectra.

The assignments of the infrared bands are in concert with the well-established correlation between the band positions and the type of interaction between the pyridine and the sites on which it is adsorbed. The original work with pyridine adsorbed on solid acids was done by Parry (*39*). A compilation of the various band assignments with this technique has been given by Pichat *et al.* (*40*). The band assignments are from the original work on liquid pyridine by Kline and Turkevich (*41*). Liquid pyridine, pyridine hydrogen-bonded to a surface, chemisorbed to a Lewis acid site, and chemisorbed to a Brønsted acid site all show distinctly different regions of absorption in the infrared.

RESULTS

The results of the gravimetric adsorption measurements of pyridine for all the samples are summarized in Fig. 1. Each system will be discussed separately with reference to this composite figure.

Silica. Silica without any added cations adsorbs little to no pyridine. The weight change measurement is barely within the limit of detectability. It should be noted that this is the amount of chemisorption at a pressure of pyridine of 3×10^{-5} Torr. The amount of pyridine chemisorbed at 423 K at this pressure is only 2% of the total amount

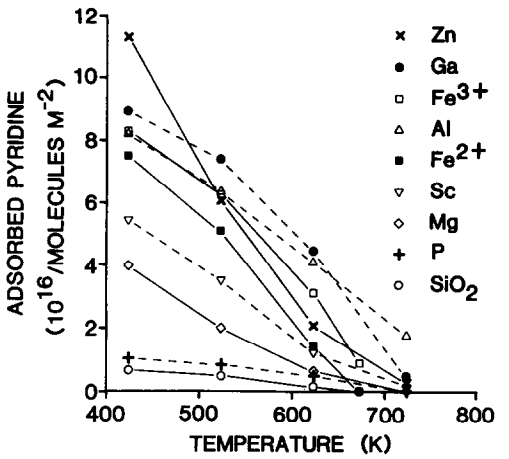

FIG. 1. Results of gravimetric adsorption measurements for pyridine adsorbed on (X) Zn/SiO_2; (●) Ga/SiO_2; (□) Fe^{3+}/SiO_2, Ref. (*34*); (△) Al/SiO_2; (■) Fe^{2+}/SiO_2, Ref. (*34*); (▽) Sc/SiO_2; (◇) Mg/SiO_2; (+) P/SiO_2; (○) SiO_2, Ref. (*34*).

adsorbed at 423 K at a pyridine pressure of 4.8 Torr. This illustrates the large amount of physisorbed pyridine present on the surface when there is an appreciable amount of pyridine in the gas phase. The infrared spectra of pyridine adsorbed on SiO_2 treated in this manner have been shown elsewhere (*34*). Only physisorbed pyridine was observed. The pyridine had major adsorption bands at 1597 and 1446 cm^{-1}.

Scandium on silica. The least electronegative dopant used in this study was scandium. The Sc/SiO_2 sample was analyzed to have a loading of 0.55 wt% Sc, which corresponds to 18.4×10^{16} cations/m^2. Gravimetric adsorption measurements of pyridine are shown in Fig. 1. The scandium adds new acid sites on the SiO_2 surface. In terms of the adsorption at 423 K, 26% of the Sc produced new acid sites on the surface.

The results of infrared spectroscopy studies of pyridine on Sc/SiO_2 are tabulated in Table 2. The spectra show the presence of Brønsted and Lewis acid sites, as well as physisorbed or hydrogen-bonded pyridine (HPY). The first spectrum, collected after desorption of pyridine at 423 K to a pressure of 1×10^{-3} Torr, contained bands for

TABLE 2

Infrared Absorption Frequencies for Spectra of Pyridine Adsorbed on 0.55 wt% Sc/SiO_2 Shown in Figure 2

Type	Band	Evacuation temperature (K); pressure (Torr)				
		423; 1×10^{-3}	423; 2×10^{-4}	523; 1×10^{-4}	623; 1×10^{-4}	723; 1×10^{-4}
LPY	19b	1447	1448	1450	1450	1451
	19a	1492	1492	1492	1493	1494
	8b	1577	1577	1577	1576	
	8a	1609	1610	1612	1612	1612
BPY	19b	1549	1547			
	19a	1492	1492	1492		
	8b	1577	1577			
	8a	1639	1639	1640		
HPY	19b	1447				
	19a	1492				
	8b	1577				
	8a	1597				

Note. LPY = Lewis pyridine; BPY = Brønsted pyridine; HPY = physisorbed or hydrogen-bonded pyridine.

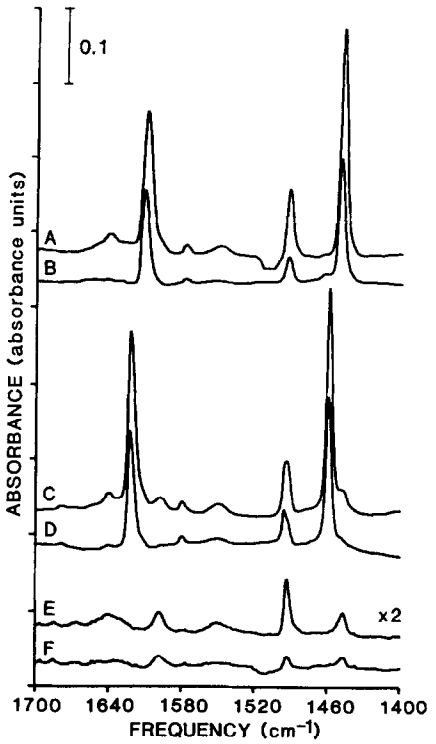

FIG. 2. Room temperature infrared spectra of pyridine adsorbed on (A) Sc/SiO_2, pyridine desorbed at 423 K, 2×10^{-4} Torr; (B) Sc/SiO_2, pyridine desorbed at 523 K, 1×10^{-4} Torr; (C) Ga/SiO_2, pyridine desorbed at 423 K, 2×10^{-4} Torr; (D) Ga/SiO_2, pyridine desorbed at 523 K, 1×10^{-4} Torr; (E) P/SiO_2, pyridine desorbed at 423 K, 2×10^{-4} Torr; (F) P/SiO_2, pyridine desorbed at 523 K, 2×10^{-4} Torr.

all three types of sites. Evacuation at the same temperature of 423 K to a pressure of 2×10^{-4} Torr led to the loss of the physisorbed or hydrogen-bonded pyridine 8a band at 1597 cm^{-1} and the 19b band at 1447 cm^{-1}. This spectrum is shown in Fig. 2A. The 8a bands for the Lewis-bonded pyridine (LPY) remained at 1610 and 1448 cm^{-1} and the bands for the Brønsted-bonded pyridine (BPY) remained at 1639 and 1547 cm^{-1}. Desorption of the pyridine at 523 K, shown in Fig. 2B, removed the bands for the Brønsted sites and shifted the 8a band for the Lewis sites to 1612 cm^{-1} and the 19b band to 1450 cm^{-1}. Further evacuation decreased the intensity and eventually removed the bands due to the Lewis acid sites.

In summary, Lewis and Brønsted sites were observed for Sc/SiO_2. The number of acid sites is low compared to the other samples studied but it is a significant fraction of the Sc atoms.

Magnesium on silica. Magnesium is also a cation with low electronegativity. The acidity of Mg/SiO_2 has been studied previously (*6, 42*). The conclusions have been that Mg produces acid sites of intermediate strength. The loading of the Mg on the sample used in the present study was 0.23 wt%, which corresponds to 14.2×10^{16} cations/m^2. Results of the gravimetric adsorption measurements are given in Fig. 1. The extent of pyridine adsorption at 423 K corresponds to 23% of the Mg cations. Thus Mg creates essentially the same number of new acid sites on silica as did Sc.

Pyridine absorption bands in the infrared are shown in Fig. 3 and Table 3 for the Mg/SiO_2 sample. Spectrum A shows the 8a band at 1610 cm^{-1} and a 19b band at 1448 cm^{-1} of a Lewis site along with the weakly bonded HPY band on silica at 1598 and 1448 cm^{-1}. Evacuation at 423 K to 2×10^{-4} Torr yields Spectrum B in which most of

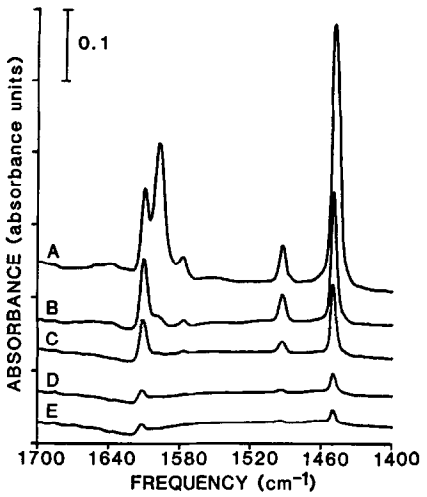

FIG. 3. Room temperature infrared spectra of pyridine adsorbed on 0.23 wt% Mg/SiO_2 after evacuation of (A) 423 K, 1×10^{-3} Torr; (B) 423 K, 2×10^{-4} Torr; (C) 523 K, 2×10^{-4} Torr; (D) 623 K, 1×10^{-4} Torr; (E) 723 K, 1×10^{-4} Torr.

the physisorbed pyridine has desorbed from the surface. As the desorption continues at higher temperatures, the 8a band shifts upward to a maximum of 1612 cm^{-1} and the 19b band shifts to 1450 cm^{-1}. There is no evidence for Brønsted acid sites on Mg/SiO_2. This series of spectra illustrates a general trend for spectra for pyridine adsorbed on Lewis acid sites. The presence of physisorbed pyridine is seen in Spectrum 3A. Evacuation at 423 K to a lower pressure confirms the assignment of the 1597-cm^{-1} band to physisorbed pyridine (Spectrum 3B). Upon continued evacuation at higher temperatures (Spectra 3C-3E), the Lewis acid bands decrease in intensity with a minor upward shift in the wavenumber of the absorption peaks.

TABLE 3

Infrared Absorption Frequencies for Spectra of Pyridine Adsorbed on 0.23 wt% Mg/SiO_2 Shown in Figure 3

Type	Band	Evacuation temperature (K); pressure (Torr)				
		423; 1×10^{-3}	423; 2×10^{-4}	523; 2×10^{-4}	623; 1×10^{-4}	723; 1×10^{-4}
LPY	19b	1448	1450	1450	1450	1450
	19a	1493	1493	1493	1493	1493
	8b	1577	1577	1576		
	8a	1610	1611	1612	1612	1612
HPY	19b	1448				
	19a	1493				
	8b	1577				
	8a	1598	1600sh			

Note. LPY = Lewis pyridine; HPY = physisorbed or hydrogen-bonded pyridine; sh = shoulder.

Iron on silica. The results for both Fe^{2+} and Fe^{3+} on silica were presented in a previous paper (*34*). The data for the gravimetric adsorption measurements are reproduced in Fig. 1. The loading of Fe is 0.52 wt%, which corresponds to 14.0×10^{16} cations/m^2. Thus, at 423 K, 50% of the Fe atoms adsorb pyridine molecules. This is a higher fraction than either Mg or Sc on SiO_2.

Infrared spectroscopy showed evidence for only Lewis acid sites on Fe/SiO_2. The absorption bands on Fe^{2+} and Fe^{3+} were observed to be at different frequencies. For divalent Fe, the 8a and 19b bands occurred at 1610 and 1451 cm^{-1}. These bands were observed after evacuation at 523 K to a pressure of 2×10^{-4} Torr. For trivalent Fe, the 8a and 19b bands occurred at 1613 and 1453 cm^{-1} after evacuation at 523 K to a pressure of 1×10^{-4} Torr.

Aluminum on silica. Silica–alumina with SiO_2 being the major component, is a classic acid catalyst. It has been shown to have strong acidity with the presence of both Lewis and Brønsted acid sites (*3, 11, 43*).

Alumina has an intermediate electronegativity of the dopants used in this study. The loading of Al on SiO_2 in the present study was 0.26 wt%, which corresponds to 14.5×10^{16} cations/m^2. The adsorption of pyridine on Al/SiO_2 is illustrated in Fig. 1. There is a large amount of pyridine that remains adsorbed after evacuation at 723 K, corresponding to strong acid sites. The amount of pyridine adsorption at 423 K is equivalent to 53% of the Al atoms, essentially the same fraction as for iron.

The existence of both Lewis and

Brønsted acid sites on Al/SiO_2 is demonstrated by the infrared data shown in Fig. 4 and Table 4. Spectrum A shows bands for three distinct pyridine adsorption sites. The first set of bands is due to physisorbed or hydrogen-bonded pyridine on SiO_2 with an 8a absorption at 1597 cm^{-1} and a 19b absorption at 1446 cm^{-1}. The second set of bands is due to Lewis sites (LPY) on Al with the 8a band at 1624 cm^{-1} and the 19b band at 1456 cm^{-1}. The third set of bands is due to Brønsted sites (BPY) with the 8a band at 1640 cm^{-1} and the 19b band at 1548 cm^{-1}. Note that the intensity of the 19a band at 1492 cm^{-1} is high in relation to the other spectra shown in this paper which contain only Lewis acid sites.

Desorption of pyridine, as seen in Spectra B–E, indicates that the physisorbed pyridine desorbs first, followed by pyridine on the Brønsted acid sites, and finally by pyridine on the Lewis acid sites. Note that there is an intense Lewis acid peak after desorption at 723 K, indicating that there are strong sites. There is also a splitting of the 19a band near 1490 cm^{-1} at the higher evacuation temperatures. The two distinct peaks are evidence that the 19a band for Brønsted and Lewis acid sites are not at the same frequency. The Lewis band is at 1497 cm^{-1} and the Brønsted band is at 1492 cm^{-1}.

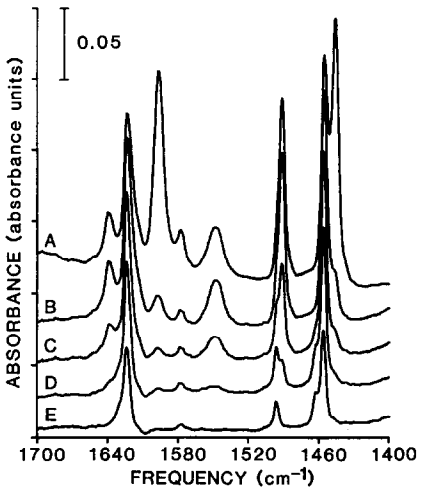

FIG. 4. Room temperature infrared spectra of pyridine adsorbed on 0.26 wt% Al/SiO_2 after evacuation at (A) 423 K, 1×10^{-3} Torr; (B) 423 K, 2×10^{-4} Torr; (C) 523 K, 1×10^{-4} Torr; (D) 623 K, 1×10^{-4} Torr; (E) 723 K, 1×10^{-4} Torr.

TABLE 4

Infrared Absorption Frequencies for Spectra of Pyridine Adsorbed on 0.26 wt% Al/SiO_2 Shown in Figure 4

Type	Band	Evacuation temperature (K); pressure (Torr)				
		423; 1×10^{-3}	423; 2×10^{-4}	523; 1×10^{-4}	623; 1×10^{-4}	723; 1×10^{-4}
LPY	19b	1456	1456	1456	1456	1457
	19a	1492	1492	1496sh	1497	1497
	8b	1578	1578	1578	1578	1577
	8a	1624	1624	1624	1625	1625
BPY	19b	1548	1547	1549		
	19a	1492	1492	1492	1492	1492
	8b	1578	1578	1578		
	8a	1640	1639	1639		
HPY	19b	1446	1446sh	1446sh		
	19a	1492	1492			
	8b	1578	1578			
	8a	1597	1597	1598		

Note. LPY = Lewis pyridine; BPY = Brønsted pyridine; HPY = physisorbed or hydrogen-bonded pyridine; sh = shoulder.

Zinc on silica. Zinc oxide has an electronegativity slightly higher than that of Al_2O_3. The Zn/SiO_2 sample prepared was analyzed to have a loading of 0.52 wt%, which corresponds to 12.0×10^{16} cations/m^2.

Pyridine adsorption data from the quartz-spring balance are depicted in Fig. 1. The adsorption at 423 K is high relative to the other dopants. This amount of adsorption corresponds to 88% of the added cations on the surface of SiO_2. Pyridine desorption is essentially complete at the 723 K evacuation.

Infrared spectroscopy indicated that all of the acid sites on Zn/SiO_2 were of the Lewis type. The absorption frequencies are listed in Table 5. In short, the spectra had the same qualitative features for pyridine adsorbed on Lewis acid sites and physisorbed pyridine as presented in Fig. 3 for Mg/SiO_2. The 8a band for chemisorbed pyridine was at 1611 cm^{-1} and the 19b band

TABLE 5

Infrared Absorption Frequencies for Spectra of Pyridine Adsorbed on 0.52 wt% Zn/SiO_2

Type	Band	Evacuation temperature (K); pressure (Torr)				
		423; 7×10^{-4}	423; 2×10^{-4}	523; 2×10^{-4}	623; 1×10^{-4}	723; 1×10^{-4}
LPY	19b	1453	1453	1454	1455	1454
	19a	1491	1491	1491	1492	1492
	8b	1578	1578	1578	1578	1578
	8a	1611	1611	1614	1614	1614
HPY	19b	1446sh	1446sh			
	19a	1491	1491			
	8b	1578	1578			
	8a	1598	1598sh			

Note. LPY = Lewis pyridine; HPY = physisorbed or hydrogen-bonded pyridine; sh = shoulder.

TABLE 6

Infrared Absorption Frequencies for Spectra of Pyridine Adsorbed on 0.57 wt% Ga/SiO_2 Shown in Figure 2

Type	Band	Evacuation temperature (K); pressure (Torr)				
		423; 8×10^{-4}	423; 2×10^{-4}	523; 1×10^{-4}	623; 1×10^{-4}	723; 1×10^{-4}
LPY	19b	1459	1459	1459	1459	1459
	19a	1493	1493	1495	1495	1495
	8b	1579	1579	1580	1580	1579
	8a	1623	1623	1623	1623	1623
BPY	19b	1548	1548	1549		
	19a	1493	1493			
	8b	1579	1579	1580		
	8a	1640	1640	1639		
HPY	19b	1446	1446sh			
	19a	1493				
	8b	1579				
	8a	1597	1597	1596		

Note. LPY = Lewis pyridine; BPY = Brønsted pyridine; HPY = physisorbed or hydrogen-bonded pyridine; sh = shoulder.

was at 1453 cm^{-1}. Desorption of pyridine led to an upward shift in the peak maxima to 1614 and 1454 cm^{-1} after evacuation at 723 K.

Gallium on silica. Gallium oxide is a highly electronegative compound. A loading of 0.57 wt% was measured for the Ga/SiO_2 sample, which corresponds to 12.3×10^{16} cations/m^2. Pyridine adsorption results are depicted in Fig. 1. The amount of adsorption at 423 K corresponds to 67% of the added Ga atoms. The curve approaches zero at 723 K, in contrast to Al for which pyridine remains adsorbed after evacuation at 723 K.

As with Al and Sc, the infrared spectra showed evidence for both Lewis and Brønsted acid sites, as shown in Figs. 2C and 2D and Table 6. A spectrum collected after pyridine exposure and evacuation at 423 K to a pressure of 7×10^{-4} Torr showed absorption bands for Lewis acid sites at 1623 cm^{-1} for the 8a band and 1459 cm^{-1} for the 19b band. Brønsted acid sites gave rise to bands at 1640 and 1548 cm^{-1} and the physisorbed pyridine appeared at 1597 and 1446 cm^{-1}. Desorption of the physisorbed pyridine at 423 K to a pressure of 2×10^{-4} Torr did not alter the Lewis or the Brønsted acid bands. This spectrum is shown in Fig. 2C. Desorption at 523 K reduced the intensities of the peaks due to the Brønsted sites, as seen in Fig. 2D. Evacuation at higher temperatures removed the Lewis acid bands. Note that the 19a band at 1493 cm^{-1} is broad when both types are present, and shifts to a higher frequency when only the Lewis acid bands are present. This is the same behavior as observed for the Al/SiO_2 sample.

Phosphorus on silica. Phosphorus was the final dopant used in this study. Phosphorus is a highly electronegative cation in the pentavalent state. The sample was prepared using incipient wetness with $(NH_4)H_2PO_4$. After preparation, the sample was treated in O_2 to keep the P fully oxidized. Thus there was no possibility of forming any reduced phosphorus compounds such as red phosphorus or phosphine (PH_3). The final phosphorus loading was 0.28 wt%, corresponding to 13.6×10^{16} cations/m^2.

The extent of pyridine adsorption on P/SiO_2 is shown in Fig. 1. As can be seen, there is little adsorption of pyridine on the P/SiO_2 system above that observed on SiO_2 alone. The changes observed are barely within experimental error. The number of new acid sites attributable to P is less than 3% of the added P.

The small number of acid sites is confirmed by the infrared spectra shown in Figs. 2E and F and Table 7. The initial spectrum after pyridine exposure and evacuation at 423 K to a pressure of 9×10^{-4} Torr showed bands due to physisorbed pyridine on SiO_2, with bands at 1597 and 1446 cm^{-1}. There were also bands at 1640 and 1550 cm^{-1} due to Brønsted acid sites, in addition to the large 19a peak at 1493 cm^{-1}. Desorption of the hydrogen-bonded or physisorbed pyridine at 423 K led to the spectrum shown in Fig. 2E, in which the Brønsted acid bands are present with only minor peaks for the hydrogen-bonded pyridine at 1597 and 1446 cm^{-1}. Note the high intensity of the 19a band for the Brønsted acid sites which occurs at 1492 cm^{-1} and remains until the pyridine is completely desorbed. Figure 2F was collected after evacuation at 523 K to a pressure of 2×10^{-4} Torr. Essentially all of the pyridine desorbed under these conditions.

In short, Brønsted acidity is observed on P/SiO_2 but the phosphorus does not generate Lewis acid sites. Previous work at higher loadings has shown Lewis acid sites (*4*). However, in the present study this was not observed. Hence, phosphorus is probably in a different structural environment than the other dopants. Previous work (*44*) has indicated that the phosphorus exists as an HPO_4^{2-} anion attached to the surface. This is evidenced in this work by the strong absorption of the IR beam by the sample in the region of 3100–2700 cm^{-1}, which is where these groups absorb in the IR (*44*).

TABLE 7

Infrared Absorption Frequencies for Spectra of Pyridine Adsorbed on 0.28 wt% P/SiO_2 Shown in Figure 2

Type	Band	Evacuation temperature (K); pressure (Torr)				
		423; 9×10^{-4}	423; 2×10^{-4}	523; 2×10^{-4}	623; 1×10^{-4}	723; 1×10^{-4}
BPY	19b	1550	1550			
	19a	1493	1492	1492	1492	
	8b	1578				
	8a	1640	1640			
HPY	19b	1446	1446	1446		
	19a	1493	1492			
	8b	1578				
	8a	1597	1598	1598	1598	

Note. BPY = Brønsted pyridine; HPY = physisorbed or hydrogen-bonded pyridine.

DISCUSSION

Lewis Acidity

Lewis acid sites were generated on silica by all of the dopant cations employed in this study (with the exception of phosphorus which was present as an anion, HPO_4^{2-}). The existence of Lewis acid sites for Sc^{3+}, Mg^{2+}, Fe^{2+}, Fe^{3+}, Al^{3+}, Zn^{2+}, and Ga^{3+} on SiO_2 is correctly predicted by the previously described model (*35*). In short, oxygen has a coordination number of two in silica. Thus, the charge transfer along each cation to anion bond according to Pauling's electrostatic bond strength rules is 2/2 or 1. Hence, for a 2+ cation on the silica surface, two bonds are required for charge neutrality. For a 3+ cation this number is three. It has been proposed previously (*35*) that when the cation coordination number predicted by these simple arguments is smaller than 4, then the cation may be coordinatively unsaturated and thus function as a Lewis acid site. Some borderline cases such as Ti^{4+}/SiO_2 with four bonds do show acidity (*4*) whereas others such as Fe^{3+}/Al_2O_3 do not show a large number of new acid sites. Phosphorus, on the other hand, has a charge of 5+ and the number of bonds required is five. Thus no Lewis acidity is predicted nor was observed for this system.

The infrared absorption frequencies are different for pyridine adsorbed on each of the different dopants. The absorption frequencies for the 8a band of Lewis-bonded pyridine can be interpreted in two ways. For the series of seven dopant cations on the silica surface there is a general increase in IR absorption frequency with an increase in electronegativity of the cation. We use the electronegativity scale of Sanderson (*36*) which takes into account the change in

electronegativity of a given cation with formal oxidation state. This trend can be seen for the data of the present study shown by the filled diamonds in Fig. 5. The data do not follow a smooth correlation, with Al showing a notable departure from the other values. In addition, the 8a band position for the low electronegative cations such as Sc, Mg, and Fe^{2+} are not very different. Alternatively, the data can be interpreted in the same manner described by Pohle and Fink (*4*). They interpreted their data in terms of two classes of cations: one class has an 8a absorption at 1612 ± 2 cm^{-1} and the other class has an 8a absorption at 1625 ± 5 cm^{-1}. In addition to the data of the present study, data from similar studies of silica supported cations are shown in Fig. 5. Pohle and Fink concluded that cations giving rise to the lower wavenumber band are octahedrally coordinated and the cations giving rise to the higher wavenumber band are tetrahedrally-coordinated. This interpretation is not completely consistent with the data of the present study. As is seen in Fig. 5, one can also group the present data into the two classes. However, it is known from Mössbauer spectroscopy that Fe^{2+} is not in an octahedral site (*34*). In fact, the coordination of Fe^{2+} is believed to be closer to tetrahedral; yet, its 8a band is in the low-frequency, octahedral class. In addition, zinc is an element that generally prefers tetrahedral coordination. (Zinc oxide, hydroxide, and all the halides except ZnF_2 have tetrahedrally bonded Zn. Zinc also forms seven different spinels in which it is tetrahedrally coordinated, and in willemite, Zn_2SiO_4, both Zn and Si are in tetrahedral sites (*45*).) Yet, Zn also falls in the octahedral category. In agreement with the assignment of Pohle and Fink, Al and Ga probably are tetrahedrally coordinated. In addition, as demonstrated earlier with α-Al_2O_3 and γ-Al_2O_3 (*35*), pyridine adsorbed on tetrahedral Al cations gives an IR band at 1624 cm^{-1} whereas octahedral Al cations absorb at 1616 cm^{-1}.

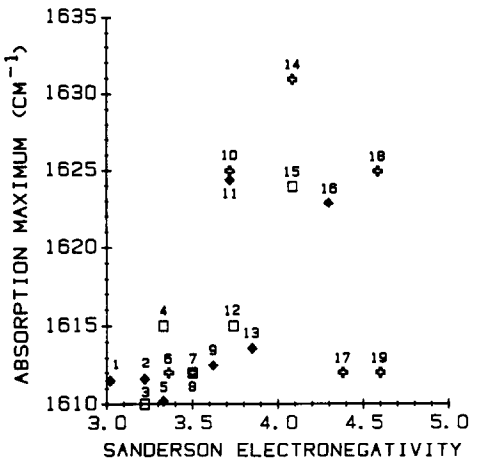

FIG. 5. Plot of the 8a absorption frequency of adsorbed pyridine versus Sanderson electronegativity for dopants on SiO_2: 1 = Sc/SiO_2; 2 = Mg/SiO_2; 3 = Mg/SiO_2, Ref. (*6*); 4 = Ni/SiO_2, Ref. (*9*); 5 = Fe^{2+}/SiO_2, Ref. (*34*); 6 = Ti/SiO_2, Ref. (*4*); 7 = Cr/SiO_2, Ref. (*4*); 8 = Cr/SiO_2, Ref. (*7*); 9 = Fe^{3+}/SiO_2, Ref. (*34*); 10 = Al/SiO_2, Ref. (*4*); 11 = Al/SiO_2; 12 = W/SiO_2, Ref. (*8*); 13 = Zn/SiO_2; 14 = B/SiO_2, Ref. (*4*); 15 = B/SiO_2, Ref. (*10*); 16 = Ga/SiO_2; 17 = Sn/SiO_2, Ref. (*4*); 18 = P/SiO_2, Ref. (*4*); 19 = Ge/SiO_2, Ref. (*4*).

In summary, the simple interpretation of the 8a band given by Pohle and Fink appears to explain much but not all of the data of the present study. A more consistent explanation cannot be presented here without additional information such as the coordination of the exposed cations, the coordination of the oxygen anions surrounding the dopant cations, and the proximity of hydroxyl groups.

As observed by Ward (*46*) and by Christner *et al.* (*47*) for ion exchanged zeolites, the frequency of the 19b band correlates with the electronegativity or electron affinity of the cation. The importance of the present study is that a series of amorphous oxides have been studied systematically so that this correlation can also be seen here. The frequencies observed vary with the evacuation treatment of the sample as well as the treatment prior to the collection of the IR spectra. Hence comparing the results of different authors can be an unreliable method of obtaining a correlation. The 19b band occurs for Lewis acid sites near

1450 cm^{-1}. The 19b band for Brønsted sites is well removed at 1540 cm^{-1}. Data reported for the 19b band must be free from physisorbed pyridine because it absorbs at wavenumbers only 5 to 10 cm^{-1} lower. The correlation of the frequency of the 19b band for the data of the present study with the Sanderson electronegativity is shown in Fig. 6. In contrast to the behavior of the 8a band, there is a more pronounced difference between the frequencies for lower electronegative elements of Sc, Mg, Fe^{2+}, and Fe^{3+}. In addition, the Fe^{2+} fits onto the smooth curve and the frequency of pyridine on Ga is higher than on Al, which is consistent with the electronegativities of these cations. The deviation of Al from the smooth curve is less than the deviation from the curve for the 8a band. In addition, the data cannot be classified into two sets as was the case for the 8a band. There is a smooth transition through all of the data as the electronegativity is increased.

In short, the changes in frequencies are not as great for the 19b band as for the 8a band, but the trends are much smoother.

It has been shown elsewhere that frequency of the 19b band for pyridine adsorbed on Lewis acid sites increases as the pyridine is more strongly bonded to the sites (*34, 35*). From this result and the data of Fig. 6, it appears that the strength of the Lewis acid sites formed by doping various cations on silica can be related to the electronegativity of the dopant cation. Thus, it is now possible to use the simple model of the previous study involving coordination arguments (*35*) to predict which dopant cations should generate Lewis acid sites on silica, and use electronegativity arguments or the frequencies of the 19b band of adsorbed pyridine to predict the relative strengths of these sites.

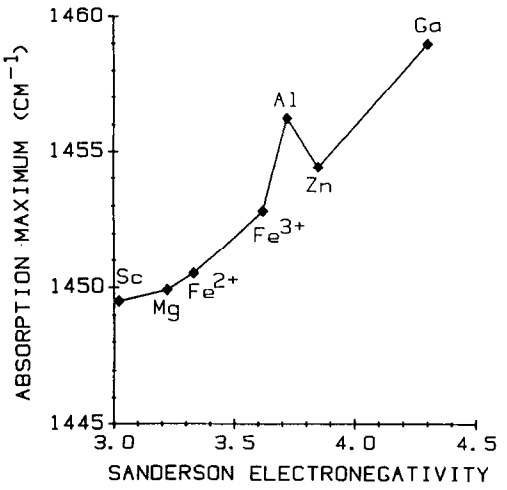

FIG. 6. Plot of the 19b absorption frequency of adsorbed pyridine versus Sanderson electronegativity for dopants on SiO_2. All samples were evacuated at 523 K to a pressure less than 2×10^{-4} Torr. Data for Fe^{2+} and Fe^{3+} from Ref. (*34*).

Brønsted Acidity

An important concept in the acidity of oxides and especially mixed oxides is the explanation of the generation of Brønsted acid sites. It is generally believed that Brønsted sites are important for such reactions as catalytic cracking and isomerization of hydrocarbons (*3*).

There have been several well-documented observations that have led to confusion about the generation of Brønsted acid sites. The first of these is that in the case of zeolites, the number of Brønsted sites can be increased upon addition of H_2O vapor with a corresponding loss of Lewis acid sites (*1–3, 47*). Thus, it has been the common conception that any strong Lewis acid sites, such as those observed on alumina, should react with H_2O to form a Brønsted acid site. However, this is not the case, as illustrated by Lercher and Noller (*42*). These authors observed a correlation between electronegativity and frequency shifts of the OH groups after adsorption of acetone. Both properties varied monotonically with the composition of the Mg/Si/Al mixed oxides. However, only Al_2O_3/SiO_2 mixtures exhibited Brønsted sites even though Mg/SiO_2 samples had the same electronegativity and the same hydroxyl-group frequency shifts.

This behavior is readily understood with reference to the generation of Brønsted acidity in zeolites. Specifically, not all of the hydroxyl groups present in the sample are Brønsted acid sites; and, instead, it is those hydroxyl groups that bridge a silicon and an aluminum cation that serve as Brønsted acid sites (*48*). The view that such bridging hydroxyl groups are the Brønsted acid sites is confirmed in calculations of the charges of protons on oxidic materials. These can be summarized by the work of Mortier and co-workers (*49, 50*). This conclusion is also in agreement with studies by Haag *et al.* (*51*) of Brønsted acid sites in ZSM-5. Their work based on magic-angle-spinning NMR as well as the kinetics of hexane cracking has shown that Al occupies a tetrahedral site. In the hydrated state the tetrahedral Al cation is in a symmetrical site with a bridging hydroxyl group between Si and Al. This bridging hydroxyl group becomes the Brønsted acid site.

The present study confirms that the above ideas about Brønsted acid sites in zeolites can be applied to mixed oxides as well, e.g., for samples prepared by doping cations onto the surface of silica. The Sc, Ga, and Al cations used in this study all have an easy bonding route using sp^3 hybrids to form tetrahedral coordination. The other cations of this study do not. That is not to say that these cations can never be forced to become Brønsted acidic. For example, Mg/SiO_2 will exhibit Brønsted acidity when prepared in such a way as to force the Mg into tetrahedral sites (*6*). However, when the sample preparation is such that only facile surface reactions occur, no Brønsted acidity is observed for these cations, such as in the present study and the studies of Noller *et al.* This concept is also confirmed by the fact that Fe generates a Brønsted acid site when it is formulated into a zeolite structure, but not when only allowed to react on the surface of silica. This is illustrated by the work of Chu and Chang (*52*).

In the present study Brønsted sites on SiO_2 were observed for Sc^{3+}, Al^{3+}, and Ga^{3+}. Note that these three cations span the range of electronegativity studied in the present work, suggesting that there is no correlation between the electronegativity of the cations and the existence of Brønsted acidity. These three cations have the same electronic configuration, have sizes similar to Si^{4+}, and they all can bond tetrahedrally through sp^3 hybrid orbitals. Thus, these trivalent cations should fit into the tetrahedral framework of SiO_2 and form a tetrahedral bond with a bridging hydroxyl group to a Si for charge neutrality. This leaves the proton available as a Brønsted acid. This proton can react with a base molecule to form a positively charged intermediate, and the solid remains in essentially the same energy state regardless of the location of the proton.

To generate this cationic Brønsted site, the dopant cation must be incorporated into the tetrahedral structure of silica. For the Sc^{3+}, Al^{3+}, and Ga^{3+} cations that exhibited Brønsted acidity, the key to the formation of this site is apparently the proper cation size and the existence of sp^3 hybrid orbitals. For example, boron supported on silica has not been found to exhibit Brønsted acidity (*4, 10*). Apparently, B^{3+} is too small to bond tetrahedrally in SiO_2 (its diameter is 25 pm compared to 40 pm for Si). Being tetrahedrally coordinated does not necessarily generate the appropriate bridging hydroxyl group. Zinc in the divalent state does not give Brønsted sites. In the 2+ oxidation state, it would produce a -2 charge if it were to be bonded in the same configuration as a 3+ cation. Addition of a second proton to balance the charge is apparently not energetically favorable. Similarly, being in the 3+ oxidation state does not guarantee that a cation will generate a Brønsted site. Transition elements such as Fe^{3+} apparently do not bond in the sp^3 tetrahedral fashion to make the proper configuration for the Brønsted acid site. This is the result of the partially filled *d* orbitals which participate in the bonding.

The above model explains cationic Brønsted sites but does not explain the Brønsted acidity observed with P. It is proposed that this is a different type of Brønsted acidity, i.e., anionic Brønsted sites. These sites are suggested to be generated by atoms (such as P, Cl, F, and S) which tend to form highly electronegative anions. There are two mechanisms commonly used to explain the generation of some types of these anionic Brønsted sites. One model is that the electron density of an OH bond is reduced by the inductive effects of the nearby electronegative anions; this weakens the OH bond and thus generates a Brønsted site (*53*). Another model is that water molecules adsorbed on the sites containing the electronegative anions form weak OH bonds which become Brønsted acid sites (*54*). Whatever the mechanism, it is proposed here that these Brønsted sites generated by highly electronegative anions are different from the Brønsted sites generated by cations substituted into the lattice of the host oxide. In general, this anionic type of Brønsted acid may be the way that many acidic supports are generated. Alumina is activated by chloride, for example, to give it the needed acidity for catalysis (*55*).

CONCLUSIONS

Lewis acid sites have been shown to be generated by doping Sc^{3+}, Mg^{2+}, Fe^{2+}, Fe^{3+}, Al^{3+}, Zn^{2+}, and Ga^{3+} onto silica. A simple model based on Pauling's electrostatic bond strength rules and cation coordination arguments has been shown to predict the presence of coordinatively unsaturated dopant cations, and thus Lewis acidity, for all of these cations on silica. Furthermore, a correlation has been found between the IR absorption frequency for the 19b band of pyridine and the electronegativity of the dopant cation. It is suggested that both of these quantities are related to the Lewis acid strength.

The existence of Brønsted acid sites has been shown to occur for Sc, Al, and Ga on silica. This is explained by a model of cationic Brønsted acids in which a tetrahedral 3+ cation substitutes into the SiO_2 matrix at the surface to produce a labile proton bonded to the surface by ionic forces. Dopant cations that bond to silica in this fashion are those which are easily forced into the tetrahedral structure as a result of their charge, size, and bonding characteristics.

A second type of Brønsted acidity, denoted as an anionic type, is produced by atoms which form highly electronegative anions. These anions can induce Brønsted acidity by other mechanisms.

ACKNOWLEDGMENTS

We thank Amoco for providing a fellowship to one of us (GC) during the course of this study. Support for this work was provided by the Office of Basic Energy Sciences of the Department of Energy (DE-FG02-84ER13183), and it is gratefully acknowledged.

REFERENCES

1. Tanabe, K., *in* "Catalysis Science and Technology" (J. R. Anderson and M. Boudart, Eds.), Vol. 2, p. 231. Springer-Verlag, New York/Berlin, 1981.
2. Tanabe, K., "Solid Acids and Bases, Their Catalytic Applications." Academic Press, New York, 1970.
3. Benesi, H. A., and Winquist, B. H. C., *in* "Advances in Catalysis" (D. D. Eley, H. Pines, and P. B. Weisz, Eds.), Vol. 27, p. 98. Academic Press, New York, 1978.
4. Pohle, W., and Fink, P., *Z. Phys. Chem. N.F.* **109,** 77 (1978).
5. Morterra, C., Ghiotti, G., Boccuzzi, F., and Coluccia, S., *J. Catal.* **51,** 299 (1978).
6. Kermarec, M., Briend-Faure, M., and Delafosse, D., *J. Chem. Soc., Faraday Trans. I* **70,** 2180 (1974).
7. Zecchina, A., Garrone, E., Ghiotti, G., and Coluccia, S., *J. Phys. Chem.* **79,** 972 (1975).
8. van Roosmalen, A. J., Koster, D., and Mol, J. C., *J. Phys. Chem.* **84,** 3075 (1980).
9. Wendt, V. G., Gottschling, J., Standte, B., and Schöllner, R., *Z. Anorg. Allg. Chem.* **500,** 215 (1983).
10. Low, M. J. D., and Subba Rao, V. V., *Canad. J. Chem.* **46,** 3255 (1968).
11. Scokart, P. O., Declerck, F. D., Sempels, R. E., and Rouxhet, P. G., *J. Chem. Soc., Faraday Trans. I* **73,** 359 (1977).

12. Scokart, P. O., and Rouxhet, P. G., *J. Coll. Int. Sci.* **86,** 96 (1982).
13. Lercher, J. A., *React. Kinet. Catal. Lett.* **20,** 409 (1982).
14. Riseman, S. M., Bandyopadhyay, S., Massoth, F. E., and Eyring, M., *Appl. Catal.* **16,** 29 (1985).
15. Lercher, J. A., Vinek, H., and Noller, H., *Appl. Catal.* **12,** 293 (1984).
16. Miyata, H., Nakagawa, Y., Ono, T., and Kubokawa, Y., *J. Chem. Soc., Faraday Trans. I* **79,** 2343 (1983).
17. Paukshtis, E. A., Soltanov, R. I., and Yurchenko, E. N., *React. Kinet. Catal. Lett.* **19,** 105 (1982).
18. Gáti, G., Halasz, I., and Resofszki, G., *Appl. Catal.* **9,** 213 (1984).
19. Morterra, C., Ghiotti, G., and Garrone, E., *J. Chem. Soc., Faraday Trans., I* **76,** 2102 (1980).
20. Parfitt, G. D., Ramsbotham, J., and Rochester, C. H., *Trans. Faraday Soc.* **67,** 1500 (1971).
21. Nakano, Y., Iizuka, T., Hattori, H., and Tanabe, K., *J. Catal.* **57,** 1 (1979).
22. Zecchina, A., Guglielminotti, E., Cerruti, L., and Coluccia, S., *J. Phys. Chem.* **76,** 571 (1972).
23. Rochester, C. H., and Topham, S. A., *J. Chem. Soc., Faraday Trans. I* **75,** 1259 (1979).
24. Busca, G., and Lorenzelli, V., *Mater. Chem.* **6,** 175 (1981).
25. Harrouche, N., Batis, H., and Ghorbel, A., *J. Chim. Phys.* **81,** 267 (1984).
26. Kayo, A., Yamaguchi, T., and Tanabe, K., *J. Catal.* **83,** 99 (1983).
27. Rochester, C. H., and Topham, S. A., *J. Chem. Soc., Faraday Trans. I* **75,** 872 (1979).
28. Parfitt, R. L., Russell, J. D., and Farmer, V. C., *J. Chem. Soc., Faraday Trans. I* **72,** 1082 (1976).
29. Morterra, C., Mirra, C., and Borello, E., *Mater. Chem. Phys.* **10,** 139 (1984).
30. Lavalley, J. C., Saussey, J., and Bovet, C., *J. Mol. Struct.* **80,** 191 (1982).
31. Morterra, C., Chiorno, A., Ghiotti, G., and Garrone, E., *J. Chem. Soc., Faraday Trans. I* **75,** 271 (1979).
32. Morrow, B. A., and Cody, I. A., *J. Phys. Chem.* **80,** 1995 (1976).
33. Harrison, P. G., and Thornton, E. W., *J. Chem. Soc., Faraday Trans. I* **71,** 1013 (1975).
34. Connell, G., and Dumesic, J. A., *J. Catal.* **101,** 103 (1986).
35. Connell., G., and Dumesic, J. A., *J. Catal.* **102,** 216 (1986).
36. Sanderson, R. T., "Inorganic Chemistry," Reinhold, New York, 1967.
37. Huheey, J. E., "Inorganic Chemistry, Principles of Structure and Reactivity," 2nd ed. Harper & Row, New York, 1978.
38. Rosynek, M. P., *Catal. Rev.-Sci. Eng.* **16,** 111 (1977).
39. Parry, E. P., *J. Catal.* **2,** 371 (1963).
40. Pichat, P., Mathieu, M.-V., and Imelik, B., *Bull. Soc. Chim. Fr.* **8,** 2611 (1969).
41. Kline, C. H., and Turkevich, J., *J. Chem. Phys.* **12,** 300 (1944).
42. Lercher, J. A., and Noller, H., *J. Catal.* **77,** 152 (1982).
43. Haw, J. F., Chuang, I-S., Hawkins, B. L., and Maciel, G. E., *J. Amer. Chem. Soc.* **105,** 7206 (1983).
44. Low, M. J. D., and Ramamurthy, P., *J. Phys. Chem.* **72,** 3161 (1968).
45. Aylett, B. J., *in* "Comprehensive Inorganic Chemistry" (A. F. Trotman-Dickens, Ed.), p. 187. Pergamon, Oxford, 1973.
46. Ward, J. W., *J. Catal.* **10,** 34 (1968).
47. Christner, L. G., Liengme, B. V., and Hall, W. K., *Trans. Faraday Soc.* **64,** 1679 (1968).
48. Uytterhoeven, J. B., Christner, L. G., and Hall, W. K., *J. Phys. Chem.* **69,** 2117 (1965).
49. Mortier, W. J., Sauer, J., Lercher, J. A., and Noller, H., *J. Phys. Chem.* **88,** 905 (1984).
50. Geerlings, P., Tariel, N., Botrel, A., Lissillour, R., and Mortier, W. J., *J. Phys. Chem.* **88,** 5752 (1984).
51. Haag, W. O., Lago, R. M., and Weisz, P. B., *Nature (London)* **309,** 589 (1984).
52. Chu, C.T-W., and Chang, C. D., *J. Phys. Chem.* **89,** 1569 (1985).
53. Ghosh, A. K., and Kydd, R. A., *Catal. Rev.-Sci. Eng.* **27,** 539 (1985).
54. Kiselev, V. F., and Krylov, O. V., "Adsorption Processes on Semiconductor and Dielectric Surfaces I," Springer Series in Chemical Physics (R. Gomer, Ed.), Vol. 32. Springer-Verlag, New York/Berlin, 1985.
55. Gates, B. C., Katzer, J. R., and Schuit, G. C. A., "Chemistry of Catalytic Processes." McGraw–Hill, New York, 1979.